Thermodynamics, kinetics and isotherm studies on the removal of methylene blue from aqueous solution by calcium alginate

Jixiang Zhang, Guangxia Zhang, Qiuxiang Zhou and Lailiang Ou

ABSTRACT

Calcium alginate (CA) was used as an adsorbent to remove methylene blue (MB) from aqueous solution. The effect of initial dye concentration, contact time, temperature and solution pH on the adsorption of MB onto CA was investigated by batch experiments. The percentage removal of MB decreased with increasing temperature. Comparatively high adsorption capacities were shown over a wide pH range (pH 2–11). More than 93% of MB removal was obtained within 30 min for an initial dye concentration of 1,000 mg/L at an adsorbent dose of 4 g/L. The adsorption equilibrium was investigated by the Langmuir and Freundlich isotherms. The maximum adsorption capacity was 2,355.4 mg/g on the basis of the Langmuir isotherm. Thermodynamic parameters were evaluated, and revealed that the adsorption process was a spontaneous, exothermic and entropy-reduced process. Pseudo-first, pseudo-second and intra-particle diffusion kinetic models were applied to the experimental data, and the results showed that the adsorption was in good agreement with the pseudo-second order kinetic model. Desorption studies implied that CA could be a useful adsorbent for the removal of MB from aqueous solution.

Key words | calcium alginate, isotherm, kinetics, methylene blue, removal, thermodynamics

Jixiang Zhang (corresponding author)
Guangxia Zhang
Qiuxiang Zhou
Department of Chemistry,
Langfang Teachers' College,
Langfang,
Hebei 065000,
China
E-mail: *zhangjixiang1973@163.com*

Lailiang Ou
Key Laboratory of Bioactive Materials of Ministry of Education,
Nankai University,
Tianjin 300071,
China

INTRODUCTION

Wastewater containing synthetic dyes from the textile, food, paper making, printing, leather and cosmetic industries may have major effects on living organisms due to the toxicity of these pollutants (Copaciu *et al.* 2013). Water bodies used to supply drinking water have become contaminated with these effluent toxicants in many developing countries. Because of its simplicity and high efficiency, adsorption technology is one of the most effective methods for the removal of organic dye pollutants, characterized by low biodegradation potential. In recent years, there has been increasing interest in the search for inexpensive and effective adsorbents, such as activated carbon produced from agricultural and industrial wastes (Bhatnagar & Sillanpää 2010), biopolymers (Sánchez-Martín *et al.* 2011), clays and clay minerals (Taha & Sadi Samaka 2012).

Sodium alginate, a biopolymer extracted from microalgae, has been recognized as a renewable, low-cost and environmentally friendly substance. Calcium alginate (CA) is a water-insoluble substance that can be produced from calcium chloride and sodium alginate. Recently, several studies have focused on the removal of heavy metal ions (Kafshgari *et al.* 2013), alkali metal ions (Ye *et al.* 2009; Wu *et al.* 2012), iodide ions (Zhang *et al.* 2011), metalloids (Dewangan *et al.* 2009; Ruiz *et al.* 2013) and rare earths (Wu *et al.* 2010) using CA and its composites as adsorbents. However, few studies have reported the removal of dyes using CA (Zhao *et al.* 2010; Sui *et al.* 2012). Methylene blue (MB), a heterocyclic aromatic cationic dye that is extensively used in the dyeing industry, was used as a model pollutant in this study. Studies on the removal of MB via adsorption from aqueous solutions by using various adsorbents have been reported previously (Sharma *et al.* 2010; Foo & Hameed 2011, 2012; Parekh *et al.* 2011; Wang *et al.* 2011; Baraka 2012; Ur Rehman *et al.* 2012; Li *et al.* 2013).

doi: 10.2166/wrd.2015.121

The aim of this study was to explore CA without any modification in order to remove MB from aqueous solutions. The effect of several operating parameters, such as initial concentration, contact time, temperature and solution pH on the adsorption were investigated by batch experiments. Equilibrium data were fitted to Langmuir and Freundlich isotherms. Adsorption kinetics models, namely pseudo-first and pseudo-second order equations and the intra-particle diffusion model, were used to examine the mechanism of the adsorption process. The thermodynamic parameters ($\triangle G^o$, $\triangle H^o$ and $\triangle S^o$) were also evaluated for the MB-CA system. In addition, a study of desorption was carried out to elucidate the possibility of recovering the adsorbent and adsorbate.

METHODS

Materials

The adsorbent used in this study, a CA powder (Lot no. AP4VJ-LT), was obtained from Tokyo Chemical Industry Co., Ltd, Japan. MB (purity, ≥98.5%) was supplied by Shanghai Hushi Chemical Co., Ltd (Shanghai, China). The molecular formula of MB is $C_{16}H_{18}ClN_3S{\cdot}3H_2O$. The structural formulae of MB and CA are shown in Figure 1. Other chemicals used were of analytical grade. All solutions were prepared using double-distilled water. The morphology of CA before and after adsorption was characterized by a scanning electron microscope (SEM; KYKY-EM3900, KYKY, China).

Preparation of dye solutions

A stock solution (10 g/L) of MB was prepared by dissolving accurately weighed amounts of MB in double-distilled water. The experimental solutions were prepared by subsequent dilution of the stock solution with distilled water. The absorbance of the MB solution after adsorption was measured at the absorption wavelength of 660 nm using a UV-visible spectrophotometer (UV-2550, Shimadzu, Japan), and the concentration of MB was calculated by using a linear calibration curve.

Adsorption experiments

To investigate the effects of the various parameters on MB adsorption by CA, all batch experiments were carried out using a model THZ-82A thermostatic water bath shaker (Ronghua, China) with a shaking speed of 110 rpm. A 25 mL solution of known dye concentration and 0.1 g of CA were added into a 150-mL Erlenmeyer flask and agitated for a given time at 25 °C, except for the study into the effect of temperature. The effect of initial concentration on MB removal was studied over a concentration range of 200–10,000 mg/L, and CA and MB solutions of various initial concentrations were agitated for 180 min. In the study into the effect of time, MB solutions with initial concentrations of 1,000, 4,000 and

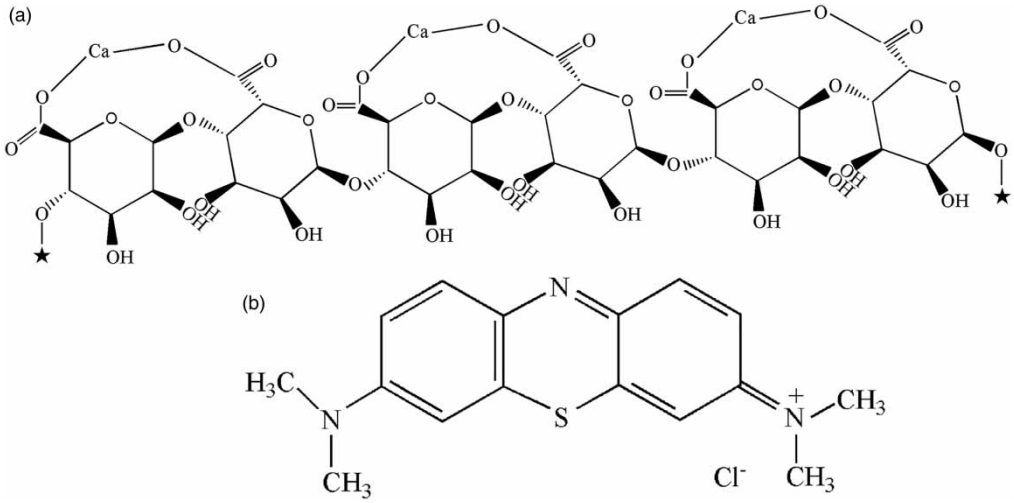

Figure 1 | Structures of a short section of CA (a) and MB (b).

10,000 mg/L and the CA adsorbent were agitated for different time intervals until adsorption equilibrium was reached. The effect of pH on MB removal was studied over a pH range of 1–11 for the 1,000 mg/L dye concentration. The pH of the solution was adjusted to a desired value by adding HCl or NaOH solution. Temperature effect batch experiments were carried out by agitating CA and MB solutions at various concentrations (1,000–10,000 mg/L) for 180 min at four different temperatures (25, 35, 45 and 55 °C) to study the thermodynamics and the adsorption isotherms. At desired times, a small amount of the supernatant was taken using a dropper and the equilibrium concentrations of MB solutions after adsorption were determined by using the linear regression equation from the calibration curve. All the adsorption experiments were conducted in duplicate.

The removal percentage ($R\%$) and the adsorption capacity (q_e, mg/g) were calculated by the following equations:

$$R\% = \frac{(C_i - C_e)}{C_i} \times 100 \quad (1)$$

$$q_e = \frac{(C_i - C_e)V}{W} \quad (2)$$

where C_i and C_e are the initial and adsorption equilibrium concentrations (mg/L) of MB solution, respectively; V is the volume of solution (L) and W is the mass (g) of the adsorbent.

Desorption studies

For desorption studies, the initial dye concentration was 1,000 mg/L. The adsorbent was separated from the dye solution by centrifugation after equilibrium. Then the spent adsorbent was transferred to an Erlenmeyer flask using 25 mL water with different pH values and agitated for 180 min. The concentrations of desorbed dye solutions were determined as mentioned before. The desorption percentage ($D\%$) was calculated by the following relationship:

$$D\% = \frac{C_d}{C_i - C_e} \times 100 \quad (3)$$

where C_d is the dye equilibrium concentration (mg/L) after desorption; C_i and C_e are as mentioned above.

RESULTS AND DISCUSSION

Characterization of CA

In Figure 2, SEM images of CA before and after adsorption show non-spherical particles of non-uniform size. Most of the particle sizes of CA before adsorption range from 50 to 80 μm, and those after adsorption are about 40 μm. The change in particle size suggests the particles of CA were aggregated before adsorption and disintegrated to smaller particles in the process of adsorption. It can be seen that the surface of CA before adsorption is rough; this uneven surface is beneficial to the removal of MB. The surface of CA becomes smooth after adsorption, indicating that the surface of the adsorbent has been coated by MB.

Effect of initial dye concentration

The effect of the initial concentration in the range 1,000–10,000 mg/L on MB removal was investigated and the

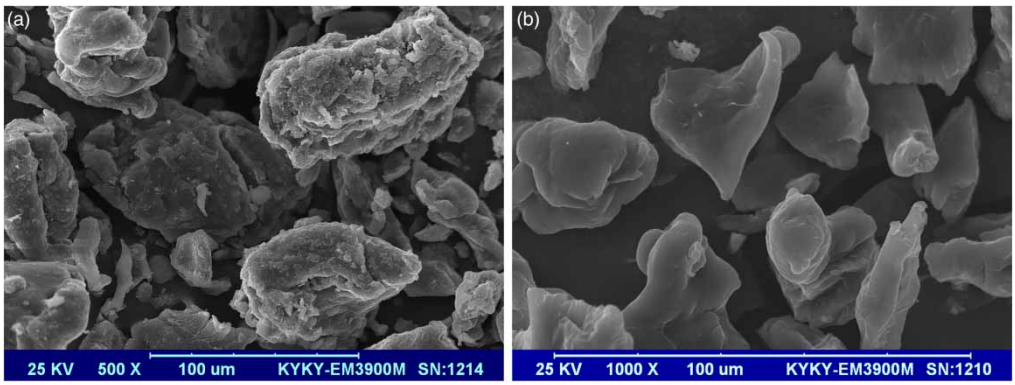

Figure 2 | SEM images of CA before (a) and after (b) adsorption.

results are presented in Figure 3. The percentage removal of MB decreased with the increase in initial concentration (2,000–10,000 mg/L). The percentage removal of MB for an initial concentration of 1,000 mg/L is approximately equal to that for 2,000 mg/L. The percentage removal was found to be 93.17% and 75.86% for 1,000 mg/L and 10,000 mg/L initial concentration, respectively. The adsorption capacity q_e was significantly affected by the initial dye concentration as well, and increased from 232.9 to 1,896.5 mg/g with the increase in MB initial concentration. The initial dye concentration provides the necessary driving force to overcome the resistance to the mass transfer of MB between the aqueous phase and the solid phase. The driving force of the concentration gradient becomes stronger and the interaction between MB and CA was enhanced as the initial concentration increased. Therefore, the adsorption capacity increases with an increase in the initial concentration of MB.

Effect of contact time

The plots of the percentage removal of MB against time for initial concentrations of 1,000, 4,000 and 10,000 mg/L are shown in Figure 4. The adsorption was rapid during the initial stages of the adsorption process. The adsorption equilibrium was reached within 30 min for the 1,000 mg/L MB solution. The equilibrium time for MB adsorption onto CA increased with an increase in the initial concentration. The adsorption equilibrium was reached after 110 min and 120 min for initial concentrations of 4,000 mg/L and

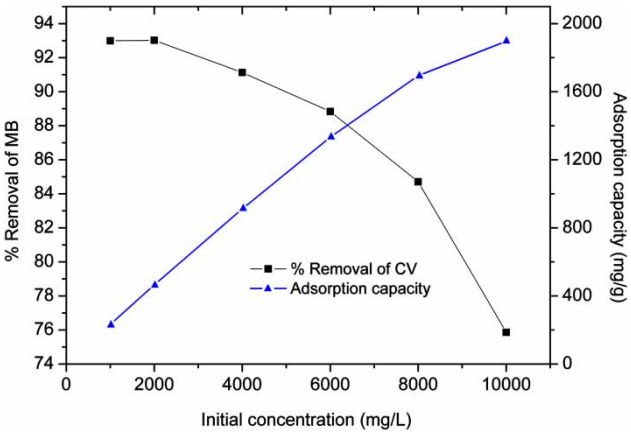

Figure 3 | Effect of initial concentration on MB removal.

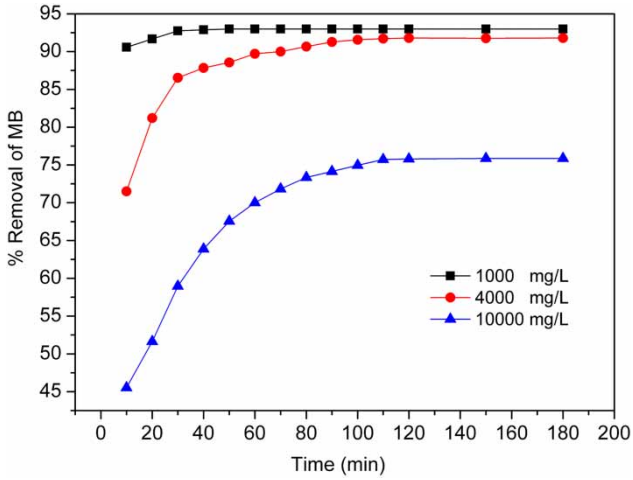

Figure 4 | Effect of contact time on MB removal.

10,000 mg/L, respectively. At the start, there were enough active sites on the surface of the CA to be occupied by the molecules of MB. As time passed, it became difficult for the adsorbent surface to be filled because of the repulsive forces among the MB molecules bound onto the CA. Moreover, it would take a longer time for the molecules of MB to diffuse into the porous structure of the CA when the surface of the CA has been saturated.

Effect of pH

To understand the adsorption mechanism, it is important to investigate the effect of solution pH on the adsorption capacity for MB. The effect of pH on dye removal was studied in the pH range of 1–11; MB solution is not stable when the pH is greater than 12. The results are shown in Figure 5. It was found that almost no adsorption was observed when the solution pH is 1, and the percentage removal increased sharply to 89.73% for the MB solution with a pH of 2. Then, a solution pH in the range of 3–11 does not have a noticeable effect on dye removal: the percentage removal of MB remains between 93.11% and 93.64% in the pH range of 3–11. A growing number of hydroxyl oxygens (O^-) would be generated from the deprotonation of hydroxyl groups (–OH) on the CA with increasing pH, which should result in an increase in the adsorption of MB onto CA due to an ion exchange process between the cationic MB and CA. However, the experimental data show that the adsorption can only vary

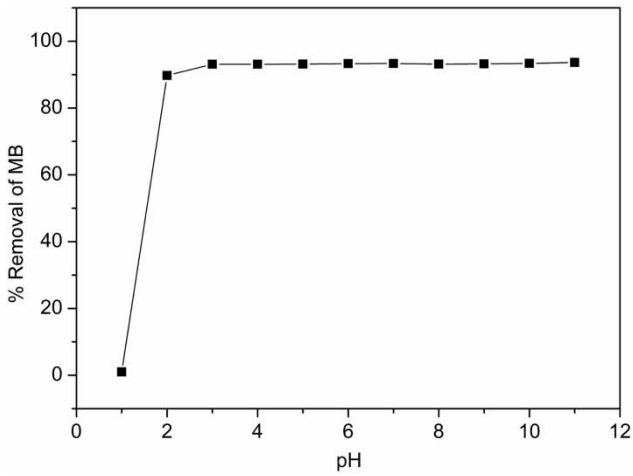

Figure 5 | Effect of pH on MB removal.

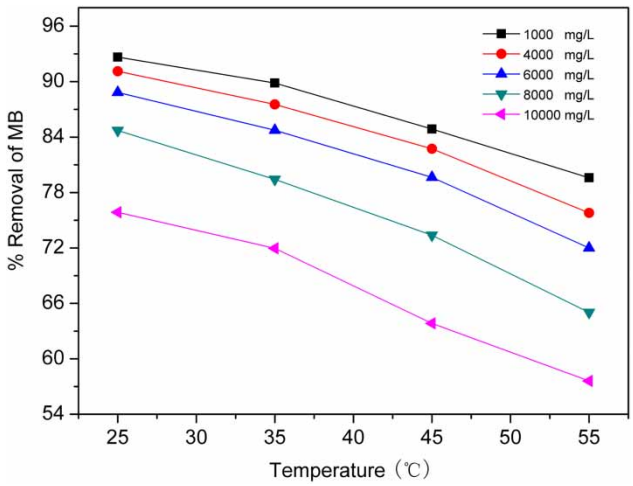

Figure 6 | Effect of temperature on MB removal.

with pH in a certain pH range. The adsorption process may also be affected by steric hindrance.

Adsorption thermodynamics

The effect of temperature from 25 to 55 °C on the removal of MB over a concentration range of 1,000 to 10,000 mg/L was investigated. The data show that the percentage removal and adsorption capacity of MB decrease with increasing temperature (Figure 6). From this trend, the decrease in the adsorption capacity at a higher temperature indicates that the adsorption of MB onto CA is an exothermic process.

The thermodynamic parameters, such as the change in Gibbs free energy (ΔG^o, kJ/mol), and the enthalpy change (ΔH^o, kJ/mol) and entropy change (ΔS^o, J·mol^{-1}·K^{-1}) for the initial concentration 1,000 mg/L, are presented in Table 1. These constants were calculated using the following equations:

$$K_c = \frac{C_{Ae}}{C_e} \tag{4}$$

$$\Delta G^o = -RT\ln K_c \tag{5}$$

$$\ln K_c = \frac{\Delta S^o}{R} - \frac{\Delta H^o}{RT} \tag{6}$$

where K_c, C_{Ae}, C_e are the equilibrium constant, the mass of MB adsorbed onto CA per liter of solution at equilibrium (mg/L) and the equilibrium concentration of MB solution (mg/L), respectively. R is the gas constant (8.314 J·mol^{-1}·K^{-1}) and T is the absolute temperature (K). A plot of lnK_c versus $1/T$ from the data in Table 1 resulted in a straight line ($R^2 = 0.9964$). The values of ΔH^o and ΔS^o are determined from the slope and the intercept, respectively, of this plot according to Equation (6). The negative values of ΔG^o and ΔH^o indicate that the adsorption of MB onto CA is a spontaneous and exothermic process. The increasing values of ΔG^o with increasing temperature suggest that the adsorption process is less favorable at higher temperature. The negative value of ΔS^o shows that the randomness at the solid CA/MB solution interface decreases during the adsorption process.

Adsorption isotherm

The study of adsorption isotherms can be used to explore how molecules of adsorbate interact with the adsorbent surface. Two important isotherms, the Langmuir (Langmuir

Table 1 | Thermodynamic parameters for adsorption of MB onto CA

Temperature (K)	Kc	ΔG^o (kJ/mol)	ΔH^o (kJ/mol)	ΔS^o (J mol^{-1} K^{-1})
298.15	12.624	−6.285	− 32.33	− 87.16
308.15	8.852	−5.587		
318.15	5.609	−4.561		
328.15	3.900	−3.713		

1918) and Freundlich (Freundlich 1906) isotherms, were tested in this work. The Langmuir isotherm model assumes a structurally homogeneous adsorbent and a monolayer coverage with no interaction between the adsorbate molecules. Compared to the Langmuir isotherm, the Freundlich isotherm model is generally more suited to the description of a heterogeneous system and a multi-layer adsorption process.

The Langmuir adsorption isotherm can be expressed as follows:

$$q_e = \frac{K_L q_m C_e}{1 + K_L C_e} \tag{7}$$

where q_e is the amount of MB adsorbed per unit mass of CA at equilibrium (mg/g); C_e is the equilibrium concentration of solution after adsorption (mg/L); K_L is the Langmuir constant (L/mg); and q_m is the maximum adsorption capacity (mg/g). The q_m and K_L values can be determined from non-linear regression analysis.

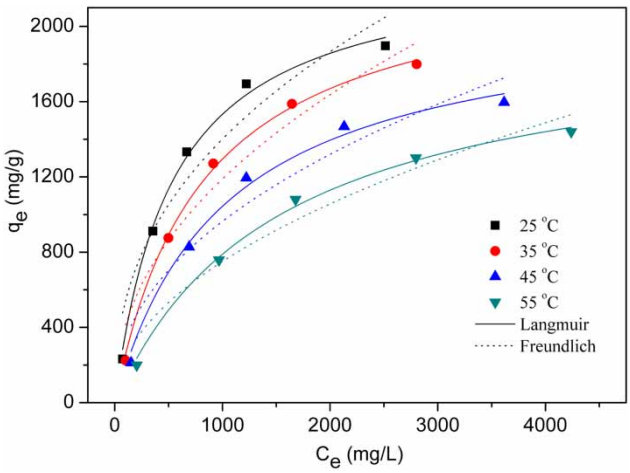

Figure 7 | Langmuir and Freundlich adsorption isotherms for the adsorption of MB onto CA.

The Freundlich adsorption isotherm is given by the following equation:

$$q_e = K_F C_e^{\frac{1}{n}} \tag{8}$$

where K_F and n are Freundlich constants reflecting the adsorption capacity at unit concentration and the adsorption intensity or surface heterogeneity, respectively. The values of K_F and n can be calculated from non-linear regression analysis.

The adsorption isotherms of MB on CA at 25, 35, 45 and 55 °C are shown in Figure 7. The values of q_m, K_L, K_F, n and the correlation coefficients (R^2) for Langmuir and Freundlich isotherm models are given in Table 2 and show that the experimental data yield excellent fits with the Langmuir model ($R^2 > 0.99$). It can be seen that the maximum monolayer adsorption capacities of CA for MB are very large in this study. This shows that the adsorption capacity is highly dependent on the chemical structures of the dye and absorbents. Consistent with the adsorption thermodynamics data, it may be seen that the adsorption is an exothermic process, with adsorption decreasing with an increase in temperature. For the Freundlich model, the most important parameter from this equation is the n value. A higher n value indicates a stronger bond between adsorbent and adsorbate. From Table 2, it is noted that the values of n are bigger than unity, reflecting that the bond between MB and CA is strong. Furthermore, the values of K_F indicate that the CA has a high adsorption capacity for MB in solution.

A comparison of the maximum adsorption capacity of MB for several adsorbents is presented in Table 3. It can be seen that the CA used in this work shows a relatively high adsorption performance for MB. Thus, CA is a promising adsorbent for the removal of MB from aqueous solution.

Table 2 | Adsorption isotherm constants for adsorption of MB onto CA

	Langmuir			Freundlich		
Temperature (°C)	K_L (L/mg)	q_m (mg/g)	R^2	K_F	n	R^2
25	1.86×10^{-3}	2,355.4	0.995	80.96	2.42	0.924
35	1.22×10^{-3}	2,351.1	0.998	49.02	2.17	0.952
45	0.98×10^{-3}	2,103.4	0.992	41.95	2.20	0.930
55	0.66×10^{-3}	1,987.4	0.996	24.75	2.02	0.955

Table 3 | Comparison of maximum adsorption of MB by other adsorbents

Adsorbents	Maximum adsorption capacity (mg/g)	Temperature (°C)	References
CA	2,355.4	25	This work
Chitosan-g-poly (acrylic acid)/ attapulgite composite	1,873	30	Wang *et al.* (2011)
Activated carbon from date stones	316.11	30	Foo & Hameed (2011)
Palm shell granular activated carbon	133.13	30	Foo & Hameed (2012)
Melamine-formaldehyde-tartaric acid resin	60.6	30	Baraka (2012)
Cocos nucifera L. activated carbon	15.59	30	Sharma *et al.* (2010)
Spent rice biomass	8.30	25	Ur Rehman *et al.* (2012)
Sodium dodecyl sulfate entrapped alginate beads	6.0530	35	Parekh *et al.* (2011)

Adsorption kinetics

In order to investigate the adsorption mechanism of MB onto CA, three of the most widely used kinetic models, i.e. pseudo-first order, pseudo-second order and the intra-particle diffusion model, have been used to fit the experimental data. The linear form of the pseudo-first order model is:

$$\log(q_{e,exp} - q_t) = \log(q_{e,cal}) - \frac{k_1}{2.303}t \quad (9)$$

where $q_{e,exp}$ is the maximum amount of dye adsorbed at equilibrium (mg/g), $q_{e,cal}$ is the calculated amount of dye adsorbed at equilibrium (mg/g) from the linear regression, q_t is amount of dye adsorbed at a time t (mg/g) and k_1 is the pseudo-first order rate constant (min^{-1}). The rate constant, k_1 and correlation coefficients R^2 of the dye at different concentrations were calculated from the linear plots of $\log(q_{e,exp}\text{-}q_t)$ versus t.

The linear form of the pseudo-second order model is as follows:

$$\frac{t}{q_t} = \frac{1}{k_2 q_{e,cal}^2} + \frac{1}{q_{e,cal}}t \quad (10)$$

where k_2 is the pseudo-second order rate constant (g/mg min) and other parameters in the relationship are the same as above. The parameters, k_2, $q_{e,cal}$, and R^2 were determined from the plots t/q_t versus t by linear regression analysis.

The intra-particle diffusion model is given by:

$$q_t = k_i t^{\frac{1}{2}} + C_i \quad (11)$$

where k_i (mg/g $min^{1/2}$) is the rate constant of intra-particle diffusion controlled sorption, and C_i (mg/g) is the intercept that characterizes the thickness of the boundary layer. The parameters, C_i and k_i can be evaluated from a linear plot of q_t versus $t^{1/2}$. Different kinetic parameters of MB adsorption onto CA for different concentrations are listed in Table 4.

From Table 4, it can be seen that the correlation coefficients (R^2) for the pseudo-first kinetic equation are not very high, between 0.912 and 0.972, indicating a poor agreement with experimental data. Moreover, the calculated values of adsorption capacity ($q_{e,cal}$) obtained from this model are significantly different from those experimental values. The result shows that the pseudo-first order kinetic model does not reflect the whole process of adsorption. In contrast, a high correlation coefficient ($R^2 > 0.999$) is obtained from the pseudo-second order model, and the values of adsorption capacity ($q_{e,cal}$) calculated from the model are also closer to those ($q_{e,exp}$) determined experimentally. This suggests that the adsorption process of MB onto CA belongs to the pseudo-second order model, indicating that the rate-limiting step might be chemical

Table 4 | Adsorption kinetic constants and correlation coefficients associated with the different kinetic models at 25 °C

	Pseudo-first order model			Pseudo-second order model				Intra-particle diffusion model		
C_i (mg/L)	k_1 (min^{-1})	$q_{e,cal}$ (mg/g)	R^2	k_2 (g/(mg·min))	$q_{e,cal}$ (mg/g)	$q_{e,exp}$ (mg/g)	R^2	k_i mg/(g·$min^{1/2}$)	C_i	R^2
1,000	0.112	21.9	0.972	2.85×10^{-2}	232.6	232.5	1.000	0.42	228.2	0.492
4,000	0.048	320.3	0.953	4.09×10^{-4}	934.6	918.0	1.000	15.72	750.2	0.673
10,000	0.047	1,824.5	0.912	5.28×10^{-5}	2,023.0	1,896.4	0.999	75.95	1,064.6	0.833

adsorption. The plots of t/q_t versus t for different initial dye concentrations are presented in Figure 8.

For the intra-particle diffusion model, all the correlation coefficients are low ($R^2 < 0.833$). According to this model, the plot of q_t versus $t^{1/2}$ should be linear if intra-particle diffusion is involved in the adsorption process. Moreover, the plots pass through the origin if intra-particle diffusion is the sole rate controlling step (Ho & Mckay 2003). It was observed that these plots do not pass through the origin, which indicates that intra-particle diffusion is not the only rate controlling step, but that other kinetic processes may also control the rate of adsorption.

Desorption studies

Desorption studies can also be used to help elucidate the mechanism of an adsorption process and to explore the possibility of recovering the adsorbent and the adsorbate. If the dye adsorbed onto the adsorbent can be desorbed by water, it can be concluded that the attachment of the dye onto the adsorbent is by weak bonds. If strong acids, such as HCl are needed to desorb the dye, it can be concluded that the attachment of the dye onto the adsorbent is by ion exchange (Mall *et al.* 2006). Water solutions with different pH values were used in the study of the desorption of MB from CA. The result is shown in Figure 9. The relatively high desorption percentage by 0.1 M HCl suggests that adsorption of MB onto CA was carried out mainly by ion exchange, which further substantiated the observations on the effect of pH on adsorption.

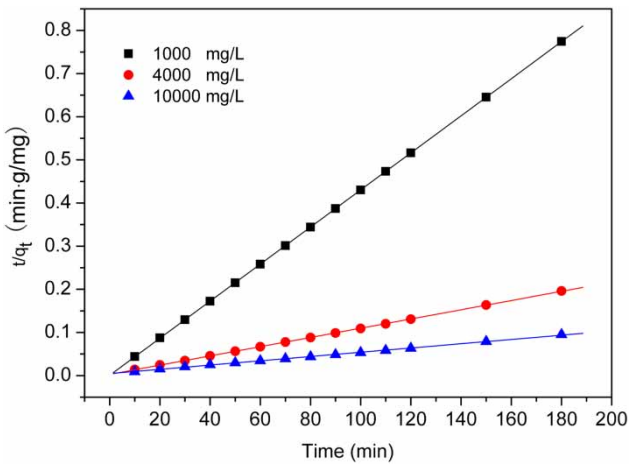

Figure 8 | Pseudo-second order for the adsorption of MB onto CA.

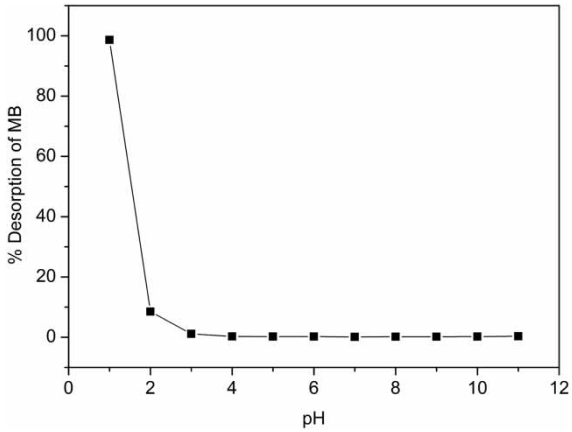

Figure 9 | Effect of pH on desorption of the MB.

CONCLUSIONS

In this study, CA was used as an adsorbent for the removal of MB from aqueous solution. The adsorption of MB depended on initial concentration, time, solution pH and temperature. An increase in initial dye concentration enhances the interaction between MB and CA, which results in an increase in adsorption capacity. The adsorption capacities of CA for MB increase with time until the adsorption equilibrium is achieved. High adsorption capacities are obtained due to ion exchange over a wide range of pH values except in high acidity solutions, such as 0.1 M HCl solution. The percentage removal of MB decreases with increasing temperature, which suggests that the adsorption of MB onto CA is an exothermic process.

An analysis of the thermodynamics for the adsorption shows the process is spontaneous and exothermic in nature. The adsorption process of MB onto CA follows the Langmuir isotherm better than the Freundlich isotherm. The maximum adsorption capacity is 2,355.4 mg/g based on the Langmuir isotherm. CA shows extraordinary adsorption capacity, which is far greater than several adsorbents reported previously. The adsorption kinetics has been assessed by the pseudo-first order, pseudo-second order and intra-particle diffusion models. It was found that the adsorption follows the pseudo-second order kinetic model for all studied concentrations, suggesting that the adsorption process is likely to be by chemisorption. In desorption studies, a relatively high desorption of MB was obtained with 0.1 M HCl solution, indicating that CA has the potential for regeneration and reuse

after MB dye adsorption. The study demonstrates that CA is an effective adsorbent for the removal of MB, and perhaps other cationic dyes, from aqueous solutions.

ACKNOWLEDGEMENTS

The authors are grateful for the financial support of the Natural Science Foundation of Hebei (No. B2015408041), the Foundation of Hebei Educational Committee (No. ZD2015079).

REFERENCES

Baraka, A. 2012 Adsorptive removal of tartrazine and methylene blue from wastewater using melamine-formaldehyde-tartaric acid resin (and a discussion about pseudo second order model). *Desalin. Water Treat.* **44**, 128–141.

Bhatnagar, A. & Sillanpää, M. 2010 Utilization of agro-industrial and municipal waste materials as potential adsorbents for water treatment – a review. *Chem. Eng. J.* **157**, 277–296.

Copaciu, F., Opriş, O., Coman, V., Ristoiu, D., Niinemets, Ü. & Copolovici, L. 2013 Diffuse water pollution by anthraquinone and azo dyes in environment importantly alters foliage volatiles, carotenoids and physiology in wheat (*Triticum aestivum*). *Water Air Soil Pollut.* **224**, 1478–1488.

Dewangan, T., Tiwari, A. & Bajpai, A. K. 2009 Removal of arsenic ions from aqueous solutions by adsorption onto biopolymeric crosslinked calcium alginate beads. *Toxico. Enviro. Chem.* **91**, 1055–1067.

Foo, K. Y. & Hameed, B. H. 2011 Preparation of activated carbon from date stones by microwave induced chemical activation: application for methylene blue adsorption. *Chem. Eng. J.* **170**, 338–341.

Foo, K. Y. & Hameed, B. H. 2012 Dynamic adsorption behavior of methylene blue onto oil palm shell granular activated carbon prepared by microwave heating. *Chem. Eng. J.* **203**, 81–87.

Freundlich, H. M. F. 1906 Over the adsorption in solution. *J. Phys. Chem.* **57**, 385–470.

Ho, Y. S. & McKay, G. 2003 Sorption of dyes and copper ions onto biosorbents. *Process Biochem.* **38**, 1047–1061.

Kafshgari, M. H., Mansouri, M., Khorram, M. & Kashani, S. R. 2013 Kinetic modeling: a predictive tool for the adsorption of zinc ions onto calcium alginate beads. *Int. J. Ind. Chem.* **4**, 5.

Langmuir, I. 1918 The adsorption of gases on plane surfaces of glass, mica and platinum. *J. Am. Chem. Soc.* **40**, 1361–1403.

Li, Y., Du, Q., Liu, T., Sun, J., Wang, Y., Wu, S., Wang, Z., Xia, Y. & Xia, L. 2013 Methylene blue adsorption on graphene oxide/calcium alginate composites. *Carbohydr. Polym.* **95**, 501–507.

Mall, I. D., Srivastava, V. C., Kumar, G. V. A. & Mishra, I. M. 2006 Characterization and utilization of mesoporous fertilizer plant waste carbon for adsorptive removal of dyes from aqueous solution. *Colloids Surf. A* **278**, 175–187.

Taha, D. N. & Sadi Samaka, I. S. 2012 Natural Iraqi palygorskite clay as low cost adsorbent for the treatment of dye containing industrial wastewater. *J. Oleo. Sci.* **61**, 729–736.

Parekh, P., Parmar, A., Chavda, S. & Bahadur, P. 2011 Modified calcium alginate beads with sodium dodecyl sulfate and clay as adsorbent for removal of methylene blue. *J. Disper. Sci. Technol.* **32**, 1377–1387.

Ruiz, M., Roset, L., Demey, H., Castro, S., Sastre, A. M. & Pérez, J. J. 2013 Equilibrium and dynamic studies for adsorption of boron on calcium alginate gel beads using principal component analysis (PCA) and partial least squares (PLS). *Materialwiss. Werkst.* **44**, 410–415.

Sánchez-Martín, J., Beltrán-Heredia, J. & Gragera-Carvajal, J. 2011 *Caesalpinia spinosa* and *Castanea sativa* tannins: a new source of biopolymers with adsorbent capacity. Preliminary assessment on cationic dye removal. *Ind. Crop. Prod.* **34**, 1238–1240.

Sharma, Y. C., Uma Sinha, A. S. K. & Upadhyay, S. N. 2010 Characterization and adsorption studies of *Cocos nucifera L.* Activated carbon for the removal of methylene blue from aqueous solutions. *J. Chem Eng. Data.* **55**, 2662–2667.

Sui, K., Li, Y., Liu, R., Zhang, Y., Zhao, X., Liang, H. & Xia, Y. 2012 Biocomposite fiber of calcium alginate/multi-walled carbon nanotubes with enhanced adsorption properties for ionic dyes. *Carbohyd. Polym.* **90**, 399–406.

Ur Rehman, M. S., Kim, I. & Han, J. I. 2012 Adsorption of methylene blue dye from aqueous solution by sugar extracted spent rice biomass. *Carbohyd. Polym.* **90**, 1314–1322.

Wang, L., Zhang, J. & Wang, A. 2011 Fast removal of methylene blue from aqueous solution by adsorption onto chitosan-g-poly (acrylic acid)/attapulgite composite. *Desalination* **266**, 33–39.

Wu, D., Zhao, J., Zhang, L., Wu, Q. & Yang, Y. 2010 Lanthanum adsorption using iron oxide loaded calcium alginate beads. *Hydrometallurgy* **101**, 76–83.

Wu, Y., Mimura, H., Niibori, Y., Ohnishi, T., Koyama, S. & Wei, Y. Z. 2012 Study on adsorption behavior of cesium using ammonium tungstophosphate (AWP)-calcium alginate microcapsules. *Sci. China Chem.* **55**, 1719–1725.

Ye, X., Wu, Z., Li, W., Liu, H., Li, Q., Qing, B., Guo, M. & Ge, F. 2009 Rubidium and cesium ion adsorption by an ammonium molybdophosphate–calcium alginate composite adsorbent. *Colloid. Surf. A* **342**, 76–83.

Zhang, H., Gao, X., Guo, T., Li, Q., Liu, H., Ye, X., Guo, M. & Wu, Z. 2011 Adsorption of iodide ions on a calcium alginate–silver chloride composite adsorbent. *Colloid Surf. A* **386**, 166–171.

Zhao, D., Shen, Y., Zhang, Y., Wei, D., Gao, N. & Gao, H. 2010 Milli-sized calcium alginate sorbent supporting the dye waste-calcium fluoride hybrid for adsorption of organic contaminants. *J. Mater. Chem.* **20**, 3098–3106.

First received 15 August 2015; accepted in revised form 1 October 2015. Available online 17 November 2015